

order stiffness constants are necessary to specify the elastic response of the crystal. In the Voigt notation, these nine independent coefficients are  $c_{11}$ ,  $c_{22}$ ,  $c_{33}$ ,  $c_{44}$ ,  $c_{55}$ ,  $c_{66}$ ,  $c_{12}$ ,  $c_{13}$ , and  $c_{23}$ . A discussion of the various orientations necessary to determine these stiffness coefficients in terms of ultrasonic waves is given by *McSkimin* [1964]. All of the on-diagonal coefficients  $c_{ii}$  may be determined from the pure mode directions parallel to the crystallographic a, b, and c axes. The three cross-coupling moduli ( $c_{12}$ ,  $c_{13}$ , and  $c_{23}$ ) may be determined from three different propagation directions perpendicular to one of the orthogonal crystallographic axes and oblique to the remaining two. The results for the adiabatic elastic stiffnesses are presented in Table 1. The sample, propagation direction  $\bar{N}$ , and polarization direction  $\bar{U}$  are also listed. In addition, the final recommended values for the various  $c_{ij}^s$  are given together with the estimated probable errors. The relations between the ultrasonic velocities, density, and individual constants have been given by *McSkimin* [1964] and *Graham* [1969].

The computations of the cross-coupling moduli depend on the direction cosines of the

propagation direction  $\bar{N}$ . Therefore, it is necessary to accurately determine the direction of propagation of the elastic ultrasonic wave. It is possible to measure the angles by the Laue technique or with an optical goniometer; however, the limiting accuracy of these methods leads to significant errors in the computed elastic moduli [*Fisher and McSkimin*, 1958]. A more accurate alternative procedure involves the determination of the angles directly from the ultrasonic data. Since each of the cross-coupling moduli may be determined by either a 'quasi-shear' (QS) or 'quasi-longitudinal' (QP) (coupled mode) elastic wave velocity, both the propagation angle and the stiffness coefficient may be simultaneously calculated. A check on the calculated propagation direction is afforded by the pure transverse mode relation. The calculated angles and the pure transverse mode cross check are indicated in Table 2.

The estimated probable errors associated with each of the stiffness coefficients in Table 1 were determined by the analysis suggested by *Fisher and McSkimin* [1958]. Tables 1 and 2 show several cross checks among the various stiffness constants. These data, however, are in-

TABLE 1. Adiabatic Elastic Stiffness Coefficients of Single-Crystal Forsterite at 25°C for the Different Propagation Directions  $\bar{N}$  and Polarization Directions  $\bar{U}$  ( $l$ ,  $m$ , and  $n$  Denote Direction Cosines)

Stiffness Coefficient	Sample	$\bar{N}$	$\bar{U}$	$c_{ij}^s$ , kb	Recommended $c_{ij}^s$ (average)
$c_{11}^s$	A	[100]	[100]	3291.1	
	B			3289.9	$3290.5 \pm 1.1$
$c_{22}^s$	A	[010]	[010]	2004.5	$2004.5 \pm 0.7$
$c_{33}^s$	A	[001]	[001]	2363.7	
	B			2362.4	$2363.1 \pm 0.8$
$c_{44}^s$	A	[010]	[001]	672.28	
	A	[001]	[010]	672.38	
	B	[001]	[010]	672.25	$672.30 \pm 0.16$
$c_{55}^s$	A	[100]	[001]	814.26	
	A	[001]	[100]	814.64	
	B	[100]	[001]	814.34	
	B	[001]	[100]	814.53	$814.44 \pm 0.20$
$c_{66}^s$	A	[100]	[010]	811.39	
	A	[010]	[100]	811.47	
	B	[100]	[010]	811.33	$811.41 \pm 0.20$
	B	[010]	[100]	811.33	
$c_{12}^s$	B	[ $lm0$ ] <sup>a</sup>		662.8	$662.8 \pm 3.6$
$c_{13}^s$	A	[ $l0n$ ] <sup>b</sup>		683.6	$683.6 \pm 9$
$c_{23}^s$	A	[ $0mn$ ] <sup>c</sup>		728.1	$728.1 \pm 4.9$

$$^a l = 0.59804, \quad m = 0.80147.$$

$$^b l = 0.84343, \quad n = 0.53723.$$

$$^c m = 0.67449, \quad n = 0.73828.$$



TABLE 2. Calculated Propagation Directions for the Cross-Coupling Stiffness Coefficients and the Associated Pure Mode Checks

Stiffness	$\bar{N}$	Angle	Pure Mode Relation	Calculated $\rho V^2$ (kbar)	Measured $\rho V^2$ (kbar)
$c_{12}^s$	$[lm0]$	$\alpha = \cos^{-1} l = 36^\circ 44'$ $\beta = \cos^{-1} m = 53^\circ 16'$	$\rho V_a^2 = l^2 c_{66}^s + m^2 c_{44}^s$	723.1	721.8
$c_{13}^s$	$[l0n]$	$\alpha = \cos^{-1} l = 32^\circ 30'$ $\gamma = \cos^{-1} n = 57^\circ 30'$	$\rho V_b^2 = l^2 c_{66}^s + n^2 c_{44}^s$	771.3	771.9
$c_{23}^s$	$[0mn]$	$\beta = \cos^{-1} m = 47^\circ 35'$ $\gamma = \cos^{-1} n = 42^\circ 25'$	$\rho V_c^2 = m^2 c_{66}^s + n^2 c_{55}^s$	813.06	813.12

## Notes.

For subscript  $a$ ,  $\bar{U} = [001]$ .For subscript  $b$ ,  $\bar{U} = [010]$ .For subscript  $c$ ,  $\bar{U} = [100]$ .

sufficient to determine the probable error in a single measurement, as the calculation of a particular modulus cannot be regarded as independent of the operations by which it was obtained. It is a more reasonable approach to estimate the possible errors involved in a particular measurement, sum up these errors, and arrive at an estimated probable error for each stiffness coefficient that can subsequently be

tested using cross-checking procedures. Considering the individual sources of error in sample thickness, orientation, density, and coupling seal effects, and extending these to estimated probable errors in the on-diagonal stiffness coefficients, the following values for  $(\Delta c_{ij}/c_{ij})$  were obtained: for the coefficients determined by longitudinal wave velocities  $\pm 0.032\%$ ; and for the coefficients determined by transverse wave velocities,  $\pm 0.024\%$ . These are estimated probable errors in percent that determine the values given in Table 1. They are seen to compare well with the deviations in the individual cross checks. Since the cross-coupling moduli involve complex expressions with various constants  $c_{ij}$  appearing explicitly with the measured velocity values, their estimated probable errors may be found from Gauss' error propagation law from the independent errors. The probable errors for the cross-coupling moduli are significantly larger than those of the on-diagonal coefficients, as would be expected.

*Pressure dependence of the elastic constants at 25°C.* The basic data used in the calculation of the pressure dependence of the various elastic moduli were the repetition delay times  $T_R$  for the possible longitudinal and transverse modes as a function of hydrostatic pressure. The data for three representative vibrational modes are plotted in Figure 1 as a function of hydrostatic pressure up to about 10 kb. In the figure, the factor  $(T_0/T_R - 1)$  is plotted for each particular mode, where  $T_0$  is the repetition delay time (two-way travel time) at atmospheric pressure, which is taken to be zero.

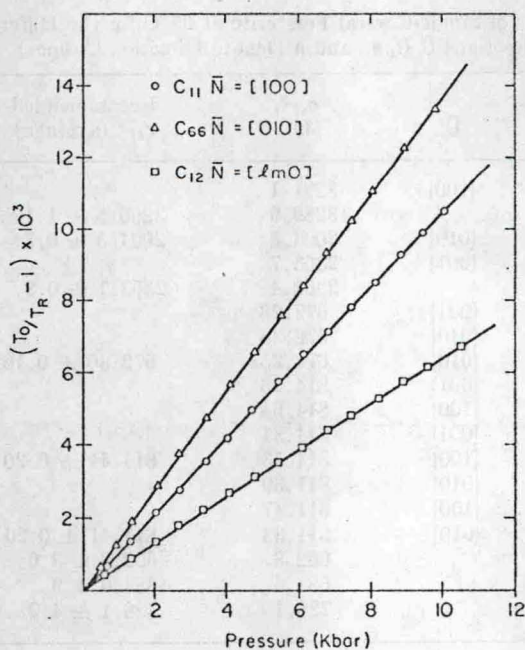


Fig. 1. Relative change of the delay time  $T_R$  as a function of pressure for three representative vibrational modes.